Autonomous Grasp of the Embedded Mobile Manipulator with an Eye-in-hand Camera

Jile Jiao, Zhiqiang Cao, Peng Zhao, Xilong Liu, Chao Zhou and Min Tan
State Key Laboratory of Management and Control for Complex Systems
Institute of Automation, Chinese Academy of Sciences
Beijing, China
{jile.jiao, zhiqiang.cao, peng.zhao, xilong.liu, chao.zhou, min.tan}@ia.ac.cn

***Abstract*—This paper proposes an autonomous grasp method for the embedded mobile manipulator with an eye-in-hand CMOS camera. A three-stage scheme including object searching, approaching and grasping operation is adopted. With the help of visual information, the Bezier curve based approaching as well as vision-based approaching adjustment is applied, where an optimal Bezier path is obtained based on the evaluation of its length and curvature with constraints from the velocity, tangential acceleration and the minimum turning radius. When the mobile manipulator thinks that the object is within its grasping range, it executes the grasping operation according to image information and inverse kinematics. During the move-to-grasp process, the posture of the manipulator is adjusted in real time to endeavor to make the object be targeted. The validity of the proposed method is verified by experiments.**

Keywords—mobile manipulator; autonomous grasp; Bezier curve; eye-in-hand

I. INTRODUCTION

Robots are today making their way into our daily life such as hospitals, offices, homes, etc [1-3]. Especially in smart home environments where the elderly and the disabled live with the help of mobile robot, there is an urgent need for the robot's manipulation ability, which may reduce independence on people and improve the quality of life. Recently, the autonomous grasp of mobile manipulator receives more and more attentions [2-4]. [1] presents a framework for the coordination and control of vehicle-arm system and discusses robotic "assistance" capabilities to aid workers in the accomplishment of a variety of physical operations, and the control method is implemented on two mobile manipulator platforms. Jain *et al.* present the assistive mobile manipulator to retrieve objects from and deliver objects to flat surfaces [2]. An algorithm for the mobile platform control is presented with maximum manipulability of the manipulator [3]. [4] presents an autonomous mobile manipulator that overcomes inherent system uncertainties and exceptions, which is demonstrated experimentally in the insertion assembly tasks. In [5], the trajectory tracking problem for a redundantly actuated omnidirectional mobile manipulator is addressed by neural network-based sliding mode method, which is demonstrated by simulation examples. [6] presents a high-precision visual control method for mobile manipulators with the abilities to maneuver itself into position, engage a target rock, etc. Minca *et al.* give a method for a robotic manipulator mounted on mobile platform applied in assembly and disassembly line, and the effectiveness is verified through experiments [7]. Jiao *et al.* propose a vision-based autonomous move-to-grasp method for a compact mobile manipulator under some low and small environments, and the mobile platform is controlled based on visual offset of the object to be grasped in the image. The effectiveness of the proposed method is verified by experiments [8]. In [9], an object grasping method based on fuzzy approaching for a mobile manipulator is proposed, and the relative angle between its heading and the object obtained from the vision information is inputted into fuzzy controller.

Generally speaking, once the object is found, object grasping operation can be decomposed into three stages: object searching, approaching and grasping. During all stages, vision is a basis for control. Among various vision systems, the eye-in-hand one has the characteristics of less error when the camera is near the object and less cover by the manipulator. [10] presents a behavior-based look-and-move control strategy for material handling of mobile manipulator, and the eye-in-hand vision system guides both the mobile base and the manipulator to perform the pick-and-place operation. Muis and Ohnishi employ a mobile manipulator as the second robot to hold the camera and propose a framework of hand-eye relation for visual servoing with precision, mobility, and global view [11].

Existing most object approaching methods about mobile manipulator with eye-in-hand vision system are reactive, and it is hard to move optimally. Bezier curve is a space curve that is smooth, continuous and derivable [12-14]. In [12], an algorithm for path planning of multiple unmanned aerial vehicles based on Bezier curve is presented, which is verified by simulation. A Bezier curve based path planning approach in a robot soccer system is proposed with consideration of the acceleration limits [13]. In this paper, we adopt Bezier curve based path planning for approaching. In addition, considering that the initial visual measurement error as well as the encoder accuracy, an extra vision-based approaching adjustment is required. The grasping operation is also divided into two separate steps: the rough grasping and the precise grasping. The former one ensures that the gripper reaches the top of the object with an assigned posture quickly, and the latter one adjusts the manipulator with the pursuit of better alignment.

The remainder of this paper is organized as follows. Section II gives the task description. Section III presents the control method. The experiment results are described in section IV and section V concludes the paper.

978-1-4799-3106-4/14/$31.00 ©2014 IEEE

II. TASK DESCRIPTION

The mobile manipulator firstly wanders in the environment to search object according to its characteristics. Once an object of interest is encountered and identified, the mobile manipulator will plan its path to approach it until the object is within the grasping range. Finally, the object is picked up. During the move-to-grasp process, the onboard manipulator is adjusted in real time to endeavor to make the object be targeted. The mobile manipulator system consists of a CMOS camera OV9653, a 6-DOF manipulator, the embedded control unit and the wheeled mobile platform, which is shown in Fig. 1. The CMOS camera is installed on the end of the arm which forms an eye-in-hand vision system. The embedded control unit mainly includes processor S3C2440A based on ARM9 and ATmega128. Also, the motor drivers, motors, two driving wheels and the universal wheel compose the wheeled mobile platform. The image is captured by the CMOS camera, and the related image information will be processed by the S3C2440 processor. With the object information and the position of the mobile manipulator, a proper path will be planned and the related command is sent to the ATmega128 and the motor drivers. ATmega128 controls the movement of the manipulator through 6 PWM signals, and the driving wheels are controlled by the motor drivers.

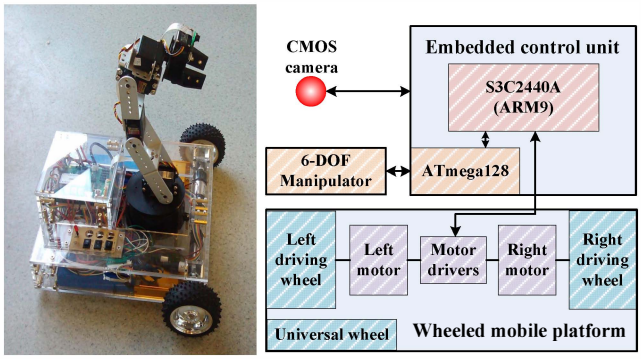

Fig. 1. The mobile manipulator system

Considering the size constraint of the compact mobile manipulator with embedded vision, we consider that the object to be grasped is slender. The accuracy and robustness of the image processing have significant effects on the vision control. In this paper, the object is endowed with a radial symbol with dual outer rings and a dual "+" symbol on the top (see Fig. 2), which may satisfy the real-time computation requirement of an embedded processor. The information of radial symbol provides the basis of Bezier path planning, whereas the dual "+" symbol is used in vision-based approaching adjustment and grasping operation. Constrained by the field of view of the camera, only a "+" symbol is used in the precise grasping.

III. CONTROL METHOD

A. Vision Information Extraction

Initially, the mobile manipulator searches the environment with the rotation of CMOS camera by adjusting the waist joint angle of the manipulator. The recognition of radial symbol is implemented in [8], and the pixel coordinates (u_r, v_r) of the radial symbol and the diameter $d_{lp}+d_{rp}$ are obtained. $O_cX_cY_cZ_c$ is established as the coordinate system of the CMOS camera, which is shown in Fig. 2. Based on the pinhole model, the position of the radial symbol in $O_cX_cY_cZ_c$ is $Y_{oc}=L*f/(d_{lp}+d_{rp})$, $X_{oc}=(u_0-u_r)*Y_{oc}/f$ and $Z_{oc}=(v_0-v_r)*Y_{oc}/f$, where L is the physical diameter of the symbol, (u_0, v_0) is the image coordinate of the intersection point of the optical axis centre line and the image plane, and f indicates the focal length in pixel. Different from the rectangle color block in [8], the dual "+" symbol is adopted to make the CMOS camera identify and match the object easily and efficiently. Similarly, the distance $D_{is}=D_{act}*f/d_{pixel}$ between the object and the CMOS camera can be acquired, where $d_{pixel}=\mathrm{sqrt}((u_1-u_2)^2+(v_1-v_2)^2)$, (u_1, v_1) and (u_2, v_2) are the pixel coordinates of centers of "+" symbols [9], and D_{act} is the physical distance between centers of "+" symbols. The position of the object in $O_cX_cY_cZ_c$ is $X'_{oc}=D_{is}*\cos\alpha$, $Y'_{oc}=D_{is}*\sin\alpha$, $Z'_{oc}=D_{is}*(u_0-(u_1+u_2)/2)/f$, where $\alpha=\theta_2+\theta_3+\theta_4$, and θ_2, θ_3 and θ_4 are pitch angles of shoulder joint, elbow joint and wrist joint, respectively. Next, the visual information is converted into the position information. As shown in Fig. 2, $O_rX_rY_rZ_r$ is established as the coordinate system of mobile platform. θ_0 and θ_1 are angles of the gripper joint and the roll joint of the wrist; θ_5 is the angle of waist joint.

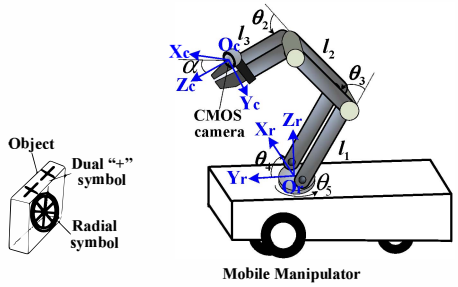

Fig. 2. The object and coordinate systems

The coordinate system $O_rX_rY_rZ_r$ rotates around its z-axis for θ_5, and x-axis for α to achieve the posture of the coordinate system $O_cX_cY_cZ_c$. Therefore, the pose matrix of camera coordinate system in the coordinate system of mobile platform can be obtained by coordinate transformation:

$$R_c^r = \begin{bmatrix} \cos\theta_5 & -\sin\theta_5 & 0 \\ \sin\theta_5 & \cos\theta_5 & 0 \\ 0 & 0 & 1 \end{bmatrix} \begin{bmatrix} 1 & 0 & 0 \\ 0 & \cos\alpha & \sin\alpha \\ 0 & -\sin\alpha & \cos\alpha \end{bmatrix} \quad (1)$$

Thus we acquire the position of the object in $O_rX_rY_rZ_r$, which is represented by $(P_{orx}, P_{ory}, P_{orz})$.

$$\begin{bmatrix} P_{orx} \\ P_{ory} \\ P_{orz} \end{bmatrix} = R_c^r \begin{bmatrix} P_{ocx} \\ P_{ocy} \\ P_{ocz} \end{bmatrix} + \begin{bmatrix} P_{crx} \\ P_{cry} \\ P_{crz} \end{bmatrix} \quad (2)$$

where $(P_{ocx}, P_{ocy}, P_{ocz})$ is the position of the object in $O_cX_cY_cZ_c$, and the position $(P_{crx}, P_{cry}, P_{crz})$ of the camera in $O_rX_rY_rZ_r$ is defined as

$$\begin{cases} P_{crx} = [l_1 \cos\theta_4 + l_2 \cos(\theta_4 + \theta_3) + l_3 \cos\alpha] \sin\theta_5 \\ P_{cry} = [l_1 \cos\theta_4 + l_2 \cos(\theta_4 + \theta_3) + l_3 \cos\alpha] \cos\theta_5 \\ P_{crz} = l_1 \sin\theta_4 + l_2 \sin(\theta_4 + \theta_3) + l_3 \sin\alpha \end{cases}, \quad (3)$$

where l_1, l_2 and l_3 are the length of the connecting rods (see Fig. 2).

When there is only one "+" symbol in the camera's view, the information we rely on is the spoke. As shown in Fig. 3, a template of recognition is introduced. Points marked "×" is scanned, and several central points (marked "o") with the pixel coordinates $(u_s,\ v_s)(s=1,\ldots,k_s)$ are obtained according to the mark points. On this basis, the slope of the spoke is $k_l=\overline{k_b}$, where k_b is determined by $(u_b,\ v_b)$ and $(u_{b+1},\ v_{b+1})(b=1,\ldots,k_s-1)$, Also, the width of the spoke in image is labeled as w_l.

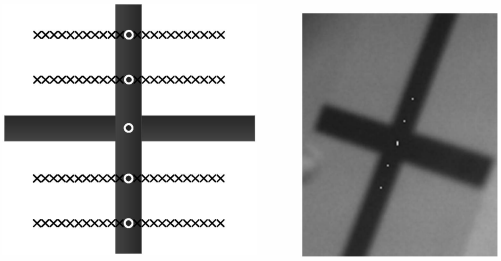

Fig. 3. Recognition template and the recognized central points on the spoke

B. The approaching of the mobile manipulator

As mentioned above, the approaching stage of the mobile platform includes two steps: Bezier curve based approaching and vision-based approaching adjustment that is implemented by endeavoring to move toward the center of the object. At the same time, the manipulator takes its proper action.

1) Bezier based path planning of the mobile platform

A Bezier curve can be represented as

$$P(\tau) = \sum_{i=0}^{n} B_{i,n}(\tau) q_i \quad 0 \le \tau \le 1 \quad (4)$$

where τ is a parameter, $B_{i,n}(\tau) = C_n^i (I-\tau)^{n-i} \tau^i$ is the Bernstein basis polynomial, n is the degree of Bernstein basis, q_i are control points. The polygon drawn through these control points is known as Bezier polygon. Bezier curves have several useful features for path planning. First, the starting point and the ending point on the curve are coincident with the first and the last control points. Second, the derivative of the starting point (τ=0) and the ending point (τ=1) of the Bezier curve is $q'(0)=n(q_1-q_0)$, $q'(1)=n(q_n-q_{n-1})$, which means that the tangential direction of the Bezier curve at starting point and ending point coincide with the polygon side q_1q_2 and $q_{n-1}q_n$, respectively.

In this paper, a cubic Bezier curve passing through four control points $q_i(x_i,\ y_i)$ $(i=0,\ldots,3)$ is adopted. Time is taken as one-dimensional variable to the solution model. $t_i(i=0,\ldots,3)$ is the time of four control points. The cubic Bezier curve is given by

$$\begin{cases} x(\tau) = \sum_{i=0}^{3} B_{i,n}(\tau) q_i = x_0(1-\tau)^3 + 3x_1\tau(1-\tau)^2 + 3x_2\tau^2(1-\tau) + x_3\tau^3 \\ y(\tau) = \sum_{i=0}^{3} B_{i,n}(\tau) q_i = y_0(1-\tau)^3 + 3y_1\tau(1-\tau)^2 + 3y_2\tau^2(1-\tau) + y_3\tau^3 \\ t(\tau) = \sum_{i=0}^{3} B_{i,n}(\tau) q_i = t_0(1-\tau)^3 + 3t_1\tau(1-\tau)^2 + 3t_2\tau^2(1-\tau) + t_3\tau^3 \end{cases} \quad (5)$$

Equation (5) can be expanded and rearranged to the form of third order polynomials about τ as

$$\begin{cases} x(\tau) = a_0 + a_1\tau + a_2\tau^2 + a_3\tau^3 \\ y(\tau) = b_0 + b_1\tau + b_2\tau^2 + b_3\tau^3 \\ t(\tau) = c_0 + c_1\tau + c_2\tau^2 + c_3\tau^3 \end{cases} \quad (6)$$

where a_i, b_i, c_i $(i=0,\ldots,3)$ are coefficients of Bezier curve which can be acquired in terms of the four control points.

According to the feature of starting point and ending point, the first control point is the current point of the mobile manipulator, and the fourth control point is near the object. According to the feature of tangential vector of Bezier curve, it is obvious that the second/third control point is on the direction of velocity of the first/fourth control point. The parameters of the first control point and the fourth control point are expressed as $P_0(x_s,\ y_s,\ t_0)$ and $P_3(x_e,\ y_e,\ t_3)$, respectively. There are $N_i=t_3/T_s$ Bezier curves planned from P_0 to P_3, where T_s is the sample time. Parameters of the second control point and the third control point of the u^{th} $(u=1,\ldots,N_i)$ Bezier path are expressed as $P_1(x_s+u\Delta d_s v_{0x},\ y_s+u\Delta d_s v_{0y},\ u\Delta d_s/v_0)$, $P_2(x_e-u\Delta d_e v_{3x},\ y_e-u\Delta d_e v_{3y},\ t_3-u\Delta d_e/v_3)$, where $v_3=v_0$; v_{0x}, v_{3x} and v_{0y}, v_{3y} are the velocities of x-axis and y-axis corresponding to v_0 and v_3, respectively. Δd_s and Δd_e are the given lengths and $\Delta d_e = \sqrt{(x_s-x_e)^2+(y_s-y_e)^2}/N_i$, $\Delta d_s=\Delta d_e/4$. All Bezier paths consist of the set Ω_b.

The Bezier path is discretized with time for the inputs of actuators. Based on the continuity and differentiability of Bezier curve, the first derivative of x, y and t to parameter τ are as follows.

$$\begin{aligned} x_\tau &= dx(\tau)/d\tau = 3a_3\tau^2 + 2a_2\tau + a_1 \\ y_\tau &= dy(\tau)/d\tau = 3b_3\tau^2 + 2b_2\tau + b_1 \\ t_\tau &= dt(\tau)/d\tau = 3c_3\tau^2 + 2c_2\tau + c_1 \end{aligned} \quad (7)$$

Hence, the velocities of x-axis and y-axis are $v_x=x_\tau/t_\tau$, $v_y=y_\tau/t_\tau$. Furthermore, the tangential accelerations are $a_{t,x}=(dv_x/d\tau)/t_\tau$, $a_{t,y}=(dv_y/d\tau)/t_\tau$. According to velocities and tangential accelerations of each point of the path, the velocities of left driving wheel v_{lw} and right driving wheel v_{rw} at each point can be acquired.

$$\begin{cases} v_{lw} = v + w_w(l_w/2) \\ v_{rw} = v - w_w(l_w/2) \end{cases} \quad (8)$$

where v=sqrt(v_x^2+ v_y^2), l_w is the distance between two driving wheels, w_w=a_t*sin($\Delta\theta$)/v is the angular velocity, a_t=sqrt($a_{t,x}^2$+ $a_{t,y}^2$), $\Delta\theta$ is the angle between the direction of the velocity and the direction of the tangential acceleration.

Considering the physical limits of mobile manipulator and the performance of the motor, the velocity, tangential acceleration and the minimum radius of turning circle of the mobile manipulator at any time must satisfy their constraints. The velocity constraint is $v \le V_{max}$. The tangential acceleration should satisfy $a_t \le A_{max}$.

The minimum radius of turning circle is R=1/κ, where $\kappa = \frac{|x_\tau y_{2\tau} - x_{2\tau} y_\tau|}{(x_\tau^2 + y_\tau^2)^{3/2}}$ is the curvature of Bezier curve, and $x_{2\tau}$=$d^2x(\tau)/d\tau^2$=$6a_3\tau$+$2a_2$, $y_{2\tau}$=$d^2y(\tau)/d\tau^2$=$6b_3\tau$+$2b_2$. And $R \ge R_{min}$.

Evaluate the path L in Ω_b using the length and curvature of the path with the consideration of the constraints mentioned above, and the optimal path L_o can be represented as:

$$\begin{aligned} L_o &= \min_{L\in\Omega_b}(k_1 \int_0^1 \sqrt{x(\tau)^2 + y(\tau)^2}\, d\tau + k_2 \int_0^1 \kappa(\tau) d\tau) \\ s.t.\quad & v \le V_{\max} \\ & a_t \le A_{\max} \\ & R \ge R_{\min} \end{aligned} \tag{9}$$

where k_1 is the weight of path length, and k_2 is the weight of curvature of the path.

2) The posture adjustment of the manipulator

When the object is localized by vision, the manipulator should be adjusted in real time to lock the object in the center of the CMOS camera, as shown in Fig. 4.

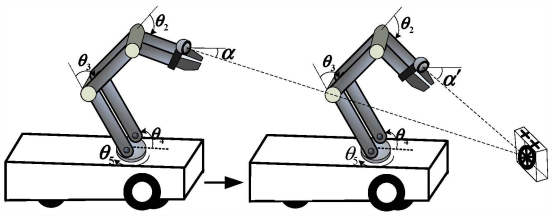

Fig. 4. Manipulator adjustment

The angle change of the horizontal direction is $\Delta\theta_5$=atan2(P_{orx}, P_{ory})−θ_5. The total angle change of the vertical direction is $\Delta\alpha$=α'−α, and each joint change is based on the left margin amount and the inertia of each connecting rod. The left margin amount of each joint is $\begin{cases} \theta_{2m} = \pi - \theta_2, \theta_{3m} = -\theta_3, \theta_{4m} = -\theta_4 \mid \Delta\alpha > 0 \\ \theta_{2m} = \theta_2, \theta_{3m} = \pi + \theta_3, \theta_{4m} = \pi + \theta_4 \mid \Delta\alpha \le 0 \end{cases}$, and the adjust amount of each joint is defined as

$$\Delta\theta_i = \Delta\alpha k_{\theta i}(\theta_{im} / \mathrm{T}_m)\ (i = 2,3,4) \tag{10}$$

where $T_m = \sum_{i=2,3,4} k_{\theta i}\theta_{im}$, $k_{\theta i}$ is the coefficient related with the inertia of each connecting rod.

When the object is out of sight in the Bezier curve based approaching step, the encoder information is used and only waist joint rotates accordingly to re-find the object while the mobile platform moves as usual. In the vision-based approaching adjustment step, the encoder information becomes less useful due to too close distance between mobile manipulator and the object. The mobile platform has to stop until the object is seen again. In this case, the manipulator searches the object, which is shown in Fig. 5, where the pitch angle θ_2 of wrist joint adopts an oscillating-type searching constrained by the manipulator and the task with an assigned interval, and θ_5 rotates from one end to another within the angle range corresponding to each θ_2. [θ_{2min}, θ_{2max}] and [θ_{5min}, θ_{5max}] are the angle ranges of θ_2 and θ_5, respectively. θ_{2s}, θ_{5s} are the joint angles of θ_2 and θ_5 at the beginning of the searching, respectively. $\Delta\theta_{2I}$ is the assigned interval of the amplitude of θ_2.

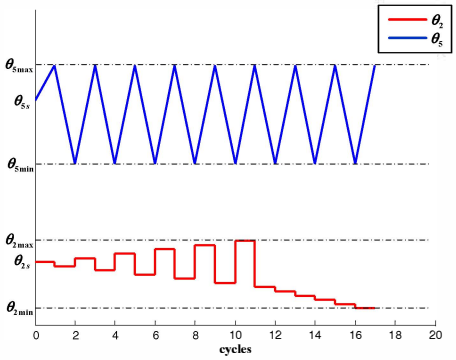

Fig. 5. Adjustment of the manipulator when the object is out of sight

C. Grasping operation

Once the object is within the reachable range of the mobile manipulator, the mobile platform stops its motion and the manipulator starts to grasp. The object searching when lost is similar to the description shown in Fig. 5.

1) Rough grasping step

This step roughly poses the gripper at the top of the object with an assigned posture based on inverse kinematics. With the consideration of the shape of the object and the gripper, the object should be grasped with the direction of the gripper almost vertical downwards. Given the constraint α=α_T. The analytic solutions of joint angels are as follows:

$$\begin{cases} \theta_2 = \alpha_T - \theta_3 - \theta_4 \\ \theta_3 = -a\cos((A^2 + B^2 - l_1^2 - l_2^2)/(2l_1l_2)) \\ \theta_4 = a\cos(\dfrac{(l_1 + l_2\cos\theta_3)A + l_2\sin\theta_3 B}{l_1^2 + l_2^2 + 2l_1l_2\cos\theta_3}) \\ \theta_5 = a\tan 2(P_{orx}, P_{ory}) \end{cases} \tag{11}$$

where A=P_{ory}/cosθ_5−l_3, B=P_{orz}.

2) Precise grasping step

After the gripper arrives at the top of the object, the roll joint angle θ_1 of wrist rotates for π/2. Then one "+" symbol is checked and grasp downwards if k_I=0 and w_I□[w_{min}, w_{max}].

IV. EXPERIMENTS

The proposed move-to-grasp method for the mobile manipulator is verified by experiments. The parameters of the method are as follows. k_s=5, T_s=0.3s, k_1=0.5, k_2=0.5, $\theta_{2\min}$= −2.8*rad*, $\theta_{2\max}$=−2.1*rad*, $\theta_{5\min}$=−0.8*rad*, $\theta_{5\max}$=0. 8*rad*, $\Delta\theta_{2f}$= 0.06*rad*, $k_{\theta 2}$=1, $k_{\theta 3}$=0, $k_{\theta 4}$=0, α_1=−π/2, w_{min}=20, w_{max}=40.

The lengths of connecting rods corresponding to the shoulder joint, elbow joint and wrist joint are l_1=95.5mm, l_2=89mm and l_3=97mm, respectively. L=109mm, f=611pixel, D_{act}=47.3mm, l_w=0.3m. v_0=0.12m/s, V_{max}=0.25m/s, A_{max}=0.04m/s^2, R_{min}=0.1m.

In experiment 1, the mobile manipulator executes a move-to-grasp task. The selected images are shown in Fig. 6, where upper three images display the approaching stage, and the lower three images describe the grasping stage with stationary mobile platform. For better description, three states are considered and they are object searching, Bezier path based approaching and vision-based approaching adjustment. Fig. 7(a) and Fig. 7(b) give the variation of joint angles and motion trajectory of the mobile platform during the approaching stage, respectively. From the experimental result, we can see that the mobile manipulator begins to execute the task from position S and it approaches the specified object after the object is observed. The posture of the manipulator is adjusted to meet the requirement of observation. When the mobile platform stops at position G, the manipulator begins to grasp and finally the task is completed.

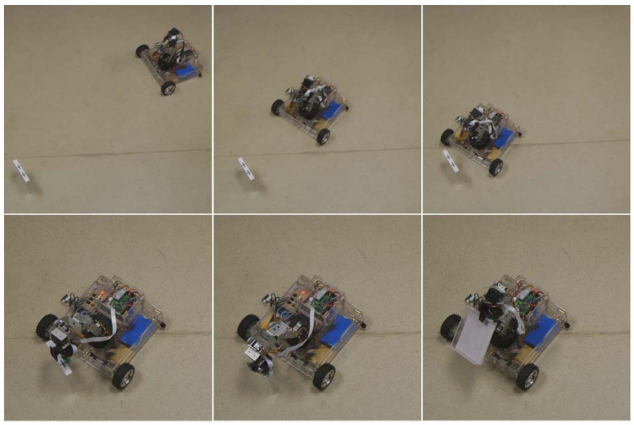

Fig. 6. A move-to-grasp operation

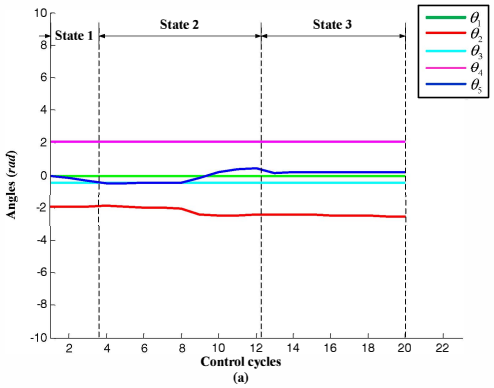

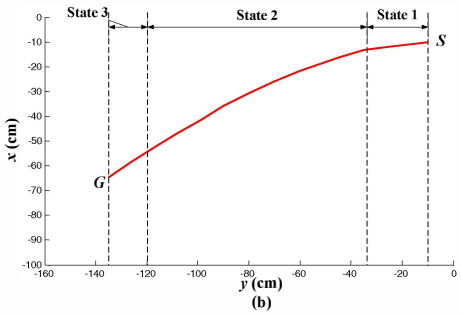

Fig. 7. The search and approaching stages of experiment 1, (a) The variation of joint angles; (b) Trajectory of the mobile platform

In experiment 2, the mobile manipulator executes a long-range move-to-grasp task. The selected images are shown in Fig. 8 and the variation of joint angles of the manipulator is shown in Fig. 9(a). The motion trajectory of the mobile platform during the approaching process is shown in Fig. 9(b), where S and G are the starting and ending positions of the mobile manipulator. It is seen that the mobile manipulator can complete the task smoothly.

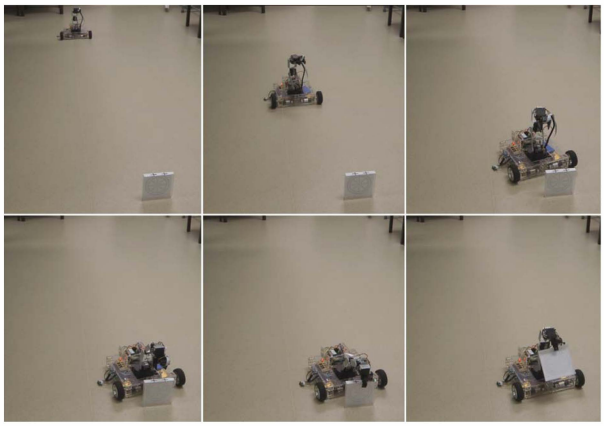

Fig. 8. A long-range move-to-grasp operation

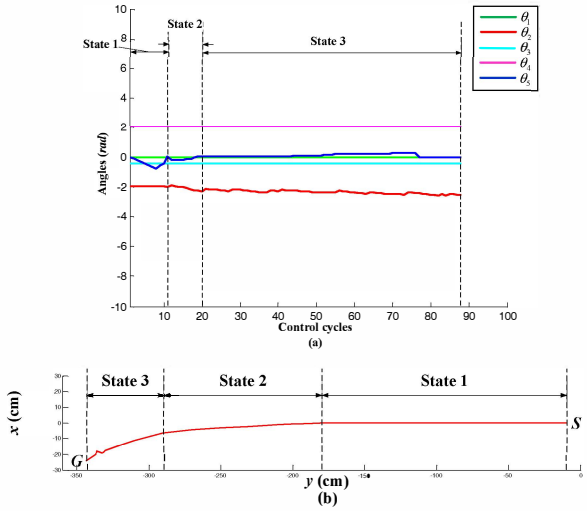

Fig. 9. The search and approaching stages of experiment 2, (a) The variation of joint angles; (b) Trajectory ofthe mobile platform

V. CONCLUSIONS

This paper proposes an autonomous grasp method for the embedded mobile manipulator with the help of an eye-in-hand CMOS camera. The whole task can be described in three stages: object searching, approaching and grasping operation. The Bezier curve based path planning is adopted for approaching, and a vision-based approaching adjustment is also added. The grasping operation is divided into the rough grasping step and the precise grasping step to achieve a better effect. The validity of the proposed method is verified by experiments. In our next work, the method will be applied into home environments with the consideration of obstacles avoidance for better environmental adaptability.

ACKNOWLEDGMENT

This work was supported in part by the National Natural Science Foundation of China under Grants 61273352, 61175111, 61227804, 60805038, 61105105. Zhiqiang Cao is the corresponding author.

REFERENCES

[1] O. Khatib, "Mobile manipulation: The robotic assistant," Robotics and Autonomous System, vol. 26, 1999, pp. 175-183.

[2] A. Jain and C. C. Kemp, "EL-E: An Assistive Mobile Manipulator that Autonomously Fetches Objects from Flat Surfaces," Autonomous Robots, vol. 28, no. 1, 2010, pp. 45-64.

[3] Y. Wang, H. X. Lang and C. W. de Silva, "A Hybrid Visual Servo Controller for Robust Grasping by Wheeled Mobile Robots," IEEE Transactions on Mechatronics, vol. 15, no. 5, 2010, pp. 757-769.

[4] B. Hamner, S. Koterba, J. Shi, R. Simmons and S. Singh, "An autonomous mobile manipulator for assembly tasks," Auton Robot, vol. 28, 2010, pp. 131-149.

[5] D. Xu, D. B. Zhao, J. Q. Yi and X. M. Tan, "Trajectory Tracking Control of Omnidirectional Wheeled Mobile Manipulator: Robust Neural Network-Based Sliding Mode Approach," IEEE Transactions on Systems, Man and Cybernetics, Part B: Cybernetics, vol. 39, no. 3, 2009, pp. 788-799.

[6] M. Seelinger, J. D. Yoder, E. T. Baumgarter and S. B. Skaar, "High-Precision Visual Control of Mobile Manipulators," IEEE Transactions on Robotics and Automation, vol. 18, no. 6, 2002, pp. 957-965.

[7] E. Minca, A. Filipescu and A. Voda, "New approach in control of assembly/disassembly line served by robotic manipulator mounted on mobile platform," Proceedings of the 2012 IEEE International Conference on Robotics and Biomimetics, Guangzhou, China, pp. 235-240.

[8] J. L. Jiao, S. G. Ye, Z. Q. Cao, N. Gu, X. L. Liu and M. Tan, "Embedded Vision Based Autonomous Move-to-Grasp for Mobile Manipulator," International Journal of Advanced Robotic Systems, vol. 9, 2012.

[9] J. L. Jiao, Z. Q. Cao, P. Zhao and M. Tan, "An Object Grasping Method Based on Fuzzy Approaching for a Mobile Manipulator", J. Huazhong Univ. of Sci. & Tech. (Natural Science Edition), vol. 41, sup. I, 2013, pp.47-50. (in Chinese)

[10] T. I. James Tsay, Y. F. Lai and Y. L. Hsiao, "Material Handling of Mobile Manipulator Using an Eye-in-Hand Vision System," The 2010 IEEE/RSJ International Conference on Intelligent Robots and Systems, October 18-22, 2010, Taipei, Taiwan, pp. 4743-4748.

[11] A. Muis and K. Ohnishi, "Eye-to-Hand approach on Eye-in-Hand configuration within real-time visual servoing," IEEE/ASME Transactions on Mechatronics, vol. 10, no. 4, 2005, pp. 404-410.

[12] F. Hu and S. Wang, "An algorithm for path planning of multiple unmanned aerial vehicles based on Bezier curve," Proceedings of the 29th Chinese Control Conference, Beijing, China, 2010, pp. 3660-3665.

[13] K. G. Jolly, R. Sreerama Kumar and R. Vijayakumar, "A Bezier curve based path planning in a multi-agent robot soccer system without violating the acceleration limits," Robotics and Autonomous Systems, vol. 57, no. 1, 2009, pp. 23-33.

[14] H. Long, H. Yashiro, H. T. N. Nejad, H. D. Quoc and M. Seiichi, "Bézier curve based path planning for autonomous vehicle in urban environment," IEEE Intelligent Vehicles Symposium, San Diego, CA, USA, 2010, pp. 1036-1042.